JTTEE5 14:196-204
DOI: 10.1361/10599630523755
1059-9630/$19.00 © ASM International

Peer Reviewed

High-Performance Nanoscale Composite Coatings for Boiler Applications

D.J. Branagan, M. Breitsameter, B.E. Meacham, and V. Belashchenko

(Submitted November 19, 2003; in revised form March 30, 2004)

In this article, we will show how unconventional nanoscale composite coatings can be formed using conventional wire-arc thermal spray systems. The as-sprayed SHS7170 wire-arc coatings are found to develop an amorphous matrix structure containing starburst-shaped boride and carbide crystallites with sizes ranging from 60 to 140 nm. After heating to temperatures above the peak crystalline temperature (566 °C), a solid/state transformation occurs that results in the formation of an intimate three-phase matrix structure consisting of the same complex boride and carbide phases, along with α-iron interdispersed on a structural scale from 60 to 110 nm. The nanocomposite microstructure contains clean grain boundaries, which are found to be extremely stable and resist coarsening throughout the range of temperatures found in boilers. Additionally, the properties of the coating are presented including the bond strength, hardness, bend resistance, and impact resistance. The sprayability, forgiveness, and repairability of the SHS7170 wire-arc coatings are explained in detail, with an emphasis on field applicability in boiler environments. The performance of the SHS7170 coatings in boiler environments is measured via elevated temperature-erosion experiments conducted at 300, 450, and 600 °C using bed ash from an operating circulating fluidized-bed combustor boiler, and the results are compared with those for existing boiler coatings.

Keywords amorphous, erosion, fireside boiler, nanocomposite, thermal spray coating

1. Introduction

Erosive high-temperature wear in boilers is one of the main causes of downtime and one of the principle engineering problems in these installations. As a result of the combustion process, the oxide particles produced have a much higher melting point than the boiler operating temperature. Thus, these particles remain intact and then become entrained into the exhaust gas, resulting in a constant bombardment of particulate matter. Maintenance costs for replacing worn pipes are very high, and the downtime associated with unscheduled breakdowns caused by the failure of exchange tubes is a source of lost revenue. The environment is also very corrosive due to a number of sources, and corrosion rates are found to increase when protective scales are removed by flowing particles (Ref 1). The coating must be protective in a wide range of conditions because, in some boilers, regions exist in which complete combustion occurs resulting in oxidizing conditions, and other regions exist where partial combustion leads to reducing environments. High sulfur content creates additional corrosion problems for coal-fired boilers, especially in boilers where lower grades of coal are used.

There are several approaches that have been used to keep boilers operating for a wide variety of applications. Weld overlays have been used on new pipe in an attempt to increase their lifetime with some success, but this process adds considerable up-front expense. Thermal spray coatings are an alternate approach that offers advantages because they allow in situ recoating of the boiler tubes with the additional ability to repair localized defects inside the boiler. The ability to recoat boilers during a scheduled outage is especially attractive because downtime can be minimized, which translates into significant operational cost savings.

Several types of thermal spray coatings are commonly used in boilers today, including nickel chrome (Ref 2, 3), iron chrome (Ref 3), TAFA 95MXC, and Inconel 625. In the thermal spray industry, there has recently been a significant effort toward the development of nanostructured coatings, although none of these materials have matured to the point where they can be economically used in boilers. Two approaches have been commonly used: the first approach is to start with heavily deformed, mechanically milled powders with micron-sized particles that have a nanoscale structure (Ref 4-10); and the second approach relies on direct spraying of either nano-sized powders (Ref 11) or nanopowder precursors (Ref 12-14). Both approaches rely on maintaining the existing nanoscale structure during spraying and subsequent impact on the substrate. However, the mechanically alloyed powder contains a high amount of internal stress, which results in rapid coarsening through recovery and recrystallization mechanisms, and the nanopowder contains an extremely high amount of external surface area that rapidly combines and sinters into coarse structures. Excessive grain growth is a limiting factor in both of these approaches and occurs at low temperatures ($T_m < 0.4$).

In this article, we introduce a new iron-base cored wire, SHS7170, which readily forms nanocomposite coatings when sprayed using the wire-arc process and exhibits a combination of properties that are superior to the existing available materials for elevated temperature boiler applications. The development of nanoscale SHS7170 coatings was achieved through a novel

D.J. Branagan, M. Breitsameter, B.E. Meacham, and **V. Belashchenko,** Institute of Nanomaterials Research and Development, The NanoSteel Company, 505 Lindsay Boulevard, Idaho Falls, ID 83402. Contact e-mail: DBranagan@nanosteelco.com.

route involving processing through a solid/solid-state transformation, which can occur either during spraying or during a secondary post-heat-treating anneal. This route to nanoscale coatings was enabled by developing alloys that readily form metallic glass structures at cooling rates in the range of thermal spray processes (i.e., 10^4 to 10^5 K/s) (Ref 15, 16). During the devitrification process, the glass precursor, when heated to its crystallization temperature, readily transforms into a nanoscale composite structure. This refinement is due to the uniform nucleation and extremely high nucleation frequency during crystallization, resulting in little time for grain growth before impingement between neighboring grains. By this route, it is possible to develop very stable nanostructures that resist coarsening at elevated temperatures (Ref 17). The chief advantage of this approach, in contrast to other approaches outlined previously, is that the feedstock material, whether cored wire for wire-arc spraying or specific powder cuts for high-velocity oxyfuel and plasma spraying, is physically identical to conventional feedstock, which eliminates the spraying problems normally associated with nanosized particulate materials and also bypasses their high cost. We believe that the ability to develop nanoscale microstructures with enhanced properties using conventional technology is revolutionary.

In this article, nanocomposite microstructures are developed while spraying SHS7170 cored wire in air with commercially available wire-arc gun systems. Additionally, in analyzing the suitability of thermal spray coatings for boiler applications, we have identified several characteristics/performance criteria that are necessary to increase the lifetime of the boiler pipes, while reducing maintenance and repair costs to extend the time interval between scheduled outages. These criteria cover the gamut from ease of application and "forgiveness" of the coating during spraying, to the integrity of the coating during service, to the repairability of the coating along with its elevated temperature erosion performance. These characteristics were evaluated in detail for the SHS7170 alloy, and the results of this research are presented.

2. Experimental Procedure

2.1 Materials

The SHS7170 alloy is a proprietary, eight-element, glass-forming alloy containing by wt.% chromium (20 to 25), molybdenum (<10), tungsten (<10), boron (<10), carbon (<5), silicon (<5), manganese (<5), and the balance iron. It was designed after extensive research over a multiyear period and contains specific atomic ratios of elements to maximize glass-forming ability, hardness, erosion resistance, and corrosion resistance.

2.2 Coating Microstructure

Twin-roll wire-arc spraying was performed on a 10.16 cm^2 coupon of mild steel using a Tafa 8835 arc gun (Praxair, Danbury, CT) under optimized conditions that were determined previously by experimentation. This 0.0762 cm thick coupon was sectioned into several smaller (2.54 cm^2) samples using a diamond saw, and they were used to conduct the following tests. Material was removed from the coating for differential scanning calorimetry (DSC) using a DTA-7 system (Perkin Elmer, Boston, MA) at a heating rate of 10 °C/min with the samples protected by oxidation through the use of flowing ultra-high-purity argon. Heat treatment was conducted on two other samples from the same original coupon. These were heat treated at 700 °C for 10 min under a high vacuum. At this temperature, any metallic glass content in the coating would completely devitrify. As-sprayed and heat-treated samples were mounted and polished to a mirror finish. Vickers microhardness measurements (HV300) were made with a 300*g* load following the protocols of ASTM E384-99 using a diamond indenter. Transmission electron microscopy (TEM) specimens were made from the other heat-treated and as-sprayed samples by first slicing with a diamond saw, dimpling, and then ion milling from two directions until perforation. TEM was performed on a JEM 2010 analytical electron microscope (JEOL, Tokyo, Japan) with an EDAX (Mahwah, NJ) energy-dispersive spectrometer (EDS) using an ultrathin window detector. Convergent beam electron diffraction (CBED) was used to analyze the crystal structure and identify the nano-sized phases.

2.3 Coating Properties

Twin-roll wire-arc spraying was done using a Praxair Tafa 8835 arc gun with and without ArcJet attachments. Using a constant 12.7 cm standoff, 0.0762 cm coatings on 2.54 × 7.62 cm mild steel substrates were sprayed at 90°, 75°, 60°, and 45° angles using a constant 90° spray angle, and 0.0762 cm coatings on 2.54 × 7.62 cm mild steel substrates were sprayed at 7.62, 10.16, 12.7, and 15.24 cm spray distances. These sprayed coupons were again sectioned into samples using a diamond saw and were used to conduct the following tests. One sample from each of them was mounted and polished. Then Vickers hardness (HV300) measurements were made as before. Another sample from each coupon was surface-treated with sandpaper before superficial 15N hardness measurements were made. The porosity was measured on the microhardness-tested samples using Image Pro Plus, version 3.0, software (Media Cybernetics, Silver Spring, MD) that was interfaced with an Epiphot 300 Nikon (Tokyo, Japan) microscope imaging system. An image of the microstructure was captured, and the software integrated the dark area in the image as porosity then calculated the percentage of porosity. The oxygen content was determined by inductively coupled plasma (ICP) chemical analysis. The deposition efficiency was determined by taking the ratio of weight gained on the coupon to the total weight of wire used to spray the coupon. Bond strength data were obtained on 2.54 cm diameter bond slugs made of 1018 steel sprayed with coatings from <0.0508 to 0.254 cm thickness. Additional 316 austenitic steel slugs were coated to a thickness of 0.0508 cm. All slugs were 2.54 cm in height according to the ASTM C633-01 standard for measuring the cohesion/bond strength of thermal spray coatings. The sprayed slugs were glued to unsprayed slug counterparts using EC-2086, a type of adhesive, and were mounted in an Instron (Norwood, MA) universal electromechanical machine after the glue cured. The machine exerted an incrementally increasing force on the slugs until failure occurred. Two 2.54 × 15.24 × 0.635 cm thick mild steel substrates were sprayed with SHS7170 to a thickness of 0.0254 cm. These samples were then bent through 180° over an anvil. Impact testing was done using an impact-testing machine (Gardner, Columbia, MD). A 5.44 kg test weight was dropped from 1.016 m in height and impacted

onto a 1.27 cm diameter impact punch. In addition, an as-sprayed 2.54 × 7.62 cm coupon, was thermally cycled prior to impact testing. The heat-treatment procedure consisted of placing the wire-arc coating in a furnace at 600 °C, holding it there for 10 min at 600 °C, and then removing it from the furnace and allowing it to air cool down to room temperature. This cycle was repeated a total of 10 times before the coupon was impact-tested.

2.4 Boiler Performance

Two new unique experimental tests were designed to simulate the real-world boiler tasks of coating repair and coating tie-in. The coating repair test procedure consisted of spraying a 2.54 × 7.62 cm 1018 steel substrate with a 0.0508 cm thick coating. Then the lower half of the coupon, starting from the masking line, was stripped off. Note that the masking line was placed at the midpoint of the coupon in a direction parallel to the 7.62 cm side. Finally, another 0.0508 cm thick coating was reapplied onto the stripped area.

The coating tie-in test procedure consisted of first masking half of a mild steel substrate. Then a 0.0508 cm thick coating was sprayed on the unmasked portion of the coupon. Finally, the masking was removed, and then a 0.0508 cm thick coating was applied on the previously masked area.

To deposit the 0.0508 cm coatings for the elevated temperature erosion studies, the following optimized parameters were used: spray distance 12.7 cm; traverse velocity 60.96 cm/s; overlapping spray pattern 0.889 cm; voltage 33 V; current 200 A; green air cap; primary air pressure 0.448 MPa; and spray head pressure 0.131 to 0.138 MPa. The erosion tests were carried out on a laboratory scale, elevated-temperature erosion tester using bed ash from an operating circulating fluidized bed combustor (CFBC) boiler as the erodent material (Ref 18).

3. Results and Discussion

3.1 Coating Microstructure

3.1.1 As-Sprayed Microstructure. Because it has not previously been shown that nanoscale structures could be developed through the low-tech wire-arc process, a detailed microstructural analysis was conducted on both the as-sprayed and the heat-treated SHS7170 coatings. In Fig. 1(b), the as-sprayed microstructure is revealed using TEM microscopy. In the TEM micrograph, the glass content is roughly estimated to be 70%, based on the area fraction imaged. The as-sprayed microstructure is characterized by a glass matrix containing starburst crystallites ranging in size from 60 to 140 nm. The precipitate phases have been tentatively identified using CBED as an $(Fe\text{-}Cr\text{-}W\text{-}Mo)_{23}C_6$-type phase and a $(Fe\text{-}Cr\text{-}Mo\text{-}W)_3B$-type phase. In the selected area diffraction pattern of Fig. 1(a), the circular rings of the amorphous phase can be seen along with isolated diffraction spots from the crystallites embedded existing in the glass. Analysis by DSC verified that the as-sprayed SHS7170 wire-arc coatings contain a significant fraction of glass, which exhibits a crystallization onset temperature of 561 °C and a peak crystallization temperature of 566 °C.

3.1.2 Heat-Treated Microstructure. One concern with conventional nanoscale materials is that they contain a high fraction of two-dimensional defect phase boundaries, which, given enough activation energy, will coarsen to larger-size scales due to their excessive interfacial free energy. Because boilers operate continuously at elevated temperatures, this potential for coarsening and the resulting deleterious changes in properties are serious concerns. To study this effect, an SHS7170 coating sample was heat-treated at 700 °C for 10 min, which represents a temperature that is high enough to cause complete crystallization and is greater than the maximum operating temperature experienced by boilers.

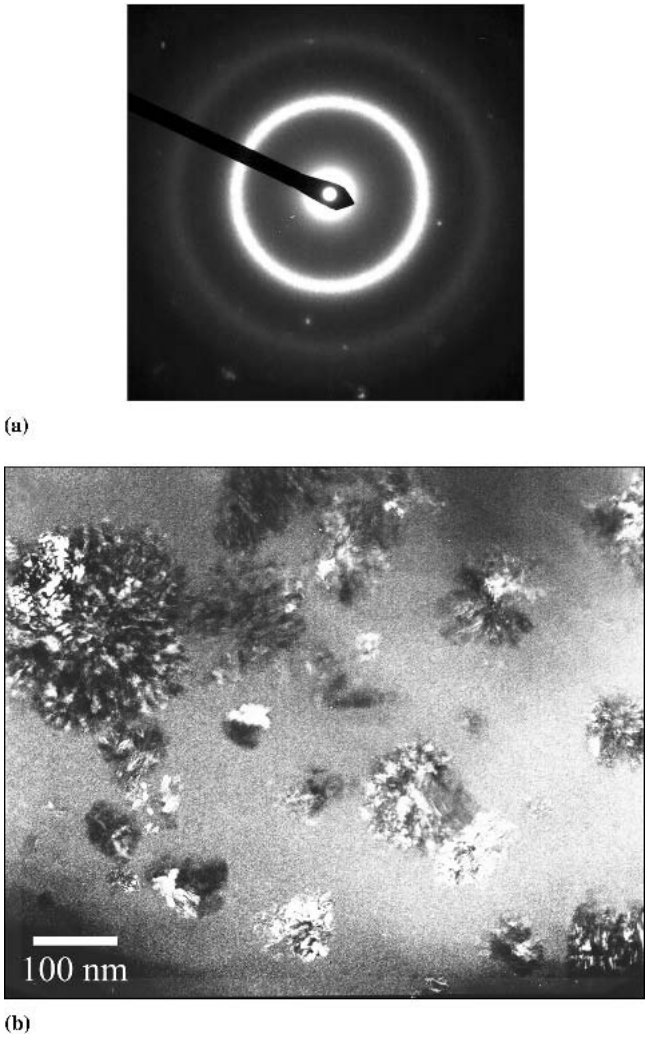

Fig. 1 Selected area diffraction (a) and TEM micrograph (b) of the as-sprayed wire-arc microstructure

Because the 700 °C heat treatment is above the peak crystallization temperature (566 °C), it can be expected that during the heat treatment the glass content would completely crystallize. The complexity of the devitrification transformation in iron-base systems has been recently described (Ref 19). The microstructure of the heat-treated SHS7170 wire-arc coatings is revealed by TEM analysis to be completely crystalline (Fig. 2b). The starburst morphology of the crystallites seen previously has transformed into a uniform equiaxed nanocomposite microstructure with phase sizes between 60 and 110 nm. Consistent

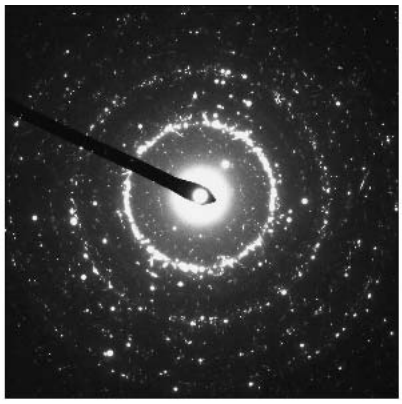

(a)

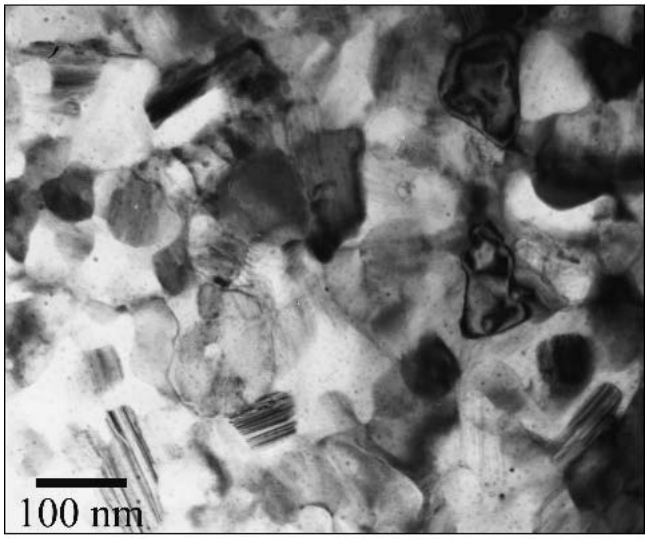

(b)

Fig. 2 Selected area diffraction (a) and TEM micrograph (b) of the SHS7170 wire-arc coating, which was heat treated at 700°C for 10 minutes

with the as-sprayed results, the microstructure was composed of three phases, consisting of αFe, a carbide phase, tentatively identified as the $(Fe\text{-}Cr\text{-}W\text{-}Mo)_{23}C_6$-type phase, and a boride phase, tentatively identified as the $(Fe\text{-}Cr\text{-}Mo\text{-}W)_3B$-type phase. The microstructure was found to consist of ≈2/3 volume fraction of nanoscale complex carbide and complex boride phases intermixed with the αFe phase. In Fig. 2(a), the selected area diffraction diagram reveals the uniform and nanoscale natures of the microstructure.

As shown after the 700 °C anneal, the microstructure of the SHS7170 wire-arc coating was found to remain nanoscale with the absence of grain coarsening. This is a characteristic of the glass devitrification process, and the formation of very stable and clean phase boundaries. Thus, one would expect that the hardness of the coating, which results to a significant extent from the achievement of the nanoscale structure, would be maintained after exposure to elevated temperatures (Ref 20). For the specific samples studied, the as-sprayed Vickers hardness (HV300) was found to be 1105 kg/mm^2, and after heat treatment the hardness increased to 1210 kg/mm^2. Thus, consistent with its microstructural stability, after being exposed to elevated temperatures, the hardness of the SHS7170 wire-arc coatings is not reduced. Furthermore, the hardness of the coating increases due to the transformation of the glass, because the hardness of the glass state is generally found to be lower than the hardness of the nanocomposite structure (Ref 15, 16, 19).

Table 1 Influence of spraying angle on properties

	Spray angle			
Property	**90°**	**75°**	**60°**	**45°**
Porosity, %	4.8	3.9	3.0	3.6
HV300	1045	1084	1166	1037
Superficial 15N	81.4	81.3	81.2	82.8
Deposit efficiency	66-69%	66-69%	66-69%	62-65%

3.2 Coating Properties

3.2.1 Porosity/Oxide Content. As indicated in Tables 1 and 2, the porosity of the SHS7170 wire-arc coatings is generally from 2% to 4% over a wide variety of spray conditions with a maximum of <5%. This represents a very low value for a wire-arc coating, and is one that maximizes boiler protection due to the minimization of permeability and interconnected porosity. One of the main reasons for this low porosity is the inherent ability of the SHS7170 alloy to resist oxidation during the spray process, which would cause the particle size and mass to increase due to the oxide scale, if oxidation were to occur, thus minimizing particle splashing and the related voids and porosity. Notice that the alloy was designed specifically to resist oxidation during spraying through a proprietary alloy design approach. The oxide content in the coatings is very low and is typically <1 vol.%. This low value is significant because oxides that are present in metallic coatings reduce the mechanical soundness of the coating, including the structural integrity and cohesive strength

The prevention of oxide formation is entirely the key to the development of nanoscale coatings because the formation of oxides in the liquid melt can result in heterogeneous nucleation sites. Once nucleation is initiated, crystallization is extremely rapid, and the resulting crystallization at low undercooling will result in the formation of phases that are several orders of magnitude larger (i.e., microscale). Only by going through the solid/solid-state glass devitrification transformation, or by just missing this regimen while undercooling to very low temperatures, can nanoscale structures be developed.

3.2.2 Bond Strength. The bond-strength tests resulted in only glue failure at 86.2 to 89.6 MPa for coatings with <0.0508 cm thickness. The results for the 0.0508 to 0.254 cm thick coatings are shown in Table 3. Clearly, the bond strengths are remarkable for wire-arc coatings and represent some of the best published values. The bond strength value of the very thick 0.254 cm sample is higher than those of most conventional materials sprayed at 0.0381 cm thickness. This is even more significant when one considers that the coatings were applied directly to the targeted base metal and no intermediate bond coat was used. While carbon steels have a wide application in boilers, for elevated boiler temperatures of >600 °C, austenitic stainless steel boiler pipes are sometimes used. The bond strength of SHS7170 wire-arc coatings were additionally measured on 316

Table 2 Influence of spray distance on properties

	Spray distance, cm			
Property	**7.62**	**10.16**	**12.7**	**15.24**
Porosity, %	3.2	3.0	4.8	3.5
HV300	1058	1072	1045	1035
Superficial 15N	84.2	83.8	81.4	81.9
Deposit efficiency	66-69%	66-69%	66-69%	62-69%

Table 3 Bond strength of SHS7170 arc-coatings as a function of thickness

Thickness, cm	0.0508	0.1016	0.1778	0.254
Bond strength, MPa	83.0	67.6	56.9	44.5

austenitic stainless steel bond slugs, and for a 0.0508 cm thick coating the bond strength was found to be very high (70.2 MPa).

To further test the bond strength of the coatings, bend testing was conducted. During the bend test, the outside of the coating is put into tension that can easily exceed the bond strength, causing cracking or delamination. Examples of two tested SHS7170 wire-arc, 0.0254 cm thick coatings are shown in Fig. 3. No cracking or delamination was observed, which underscores not only the high bond strength of the coating but also its high resiliency, which is remarkable considering its hardness.

3.2.3 Residual Stress. In conventional materials, the tensile stresses, which arise due to thermal contraction during solidification, increase as a function of coating thickness and ultimately reach a magnitude whereby the tensile stresses exceed the bond strength, resulting in coating failure from delamination. Stresses are also induced through transformations that cause a change in volume. For example, the postspray annealing of SHS7170 can cause the devitrification of the metallic glass content. It has been found that the SHS7170 wire-arc coatings have extremely low residual stresses, and no measurable bending of an as-sprayed substrate was observed on a 2.54 × 7.62 × 0.3175 cm thick carbon steel coupon when a 0.3175 cm thick coating was applied. This unique ability to spray coatings with a neutral stress condition is especially helpful for minimizing spalling during normal thermal cycles. The combination of low residual stress and very high bond strength of the SHS7170 wire-arc coatings allows the unique ability to spray very thick coatings if necessary. For example, in Fig. 4 a 20,000 μm thick coating is shown that was deposited onto a 0.635 cm thick 1018 carbon steel substrate.

3.2.4 Impact Resistance. The impact resistance of both as-sprayed and heat-treated SHS7170 wire-arc coatings sprayed to 0.0762 cm thick onto 1018 steel plate was determined. In Fig. 5, impacted coupons are shown of both the as-sprayed and thermally cycled SHS7170 wire-arc coatings after impact testing with 54.2 J of impact energy. The impact from the punch can be seen near the center of each coupon, indicating that the coating had the ability to deform during impact. On both samples, no cracking or delamination was observed, which is remarkable considering the high impact energy absorbed during the test.

3.3 Boiler Performance

Boilers are very large integrated power components that cannot be easily dissembled, moved, or taken apart. Thus, the coating of boiler components necessitates utilizing portable spray systems and applying the coatings in the field, ideally during the short time window of a scheduled maintenance or shutdown cycle. Often the conditions inside a boiler are far from ideal, with low light, tight corners, and sooty conditions, making maintenance difficult along with the additional necessity of coating the large surface area of the boiler heat-exchange pipes with a rapid

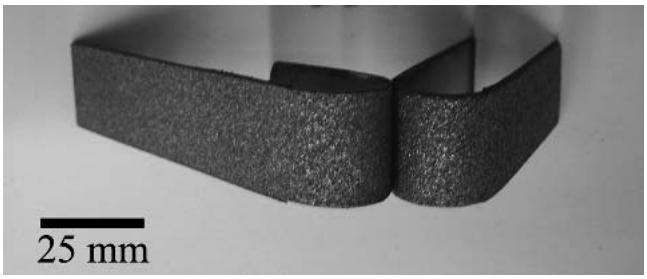

Fig. 3 Two separate wire-arc coupons with 0.0254 cm thick SHS7170 coatings, which have been bent 180°. Note that no delamination or surface cracking was observed.

Fig. 4 Optical micrograph of 20,000 μm thick SHS7170 wire-arc coating deposited onto a 0.635 cm thick 1018 plain carbon steel

Fig. 5 Example SHS7170 wire-arc coupons, (a) as-sprayed, (b) cyclic heat treated, which have been impacted with 54.2 J of impact energy during drop impact testing. Note the impact from the punch near the center of each coupon and the absence of cracking and delamination.

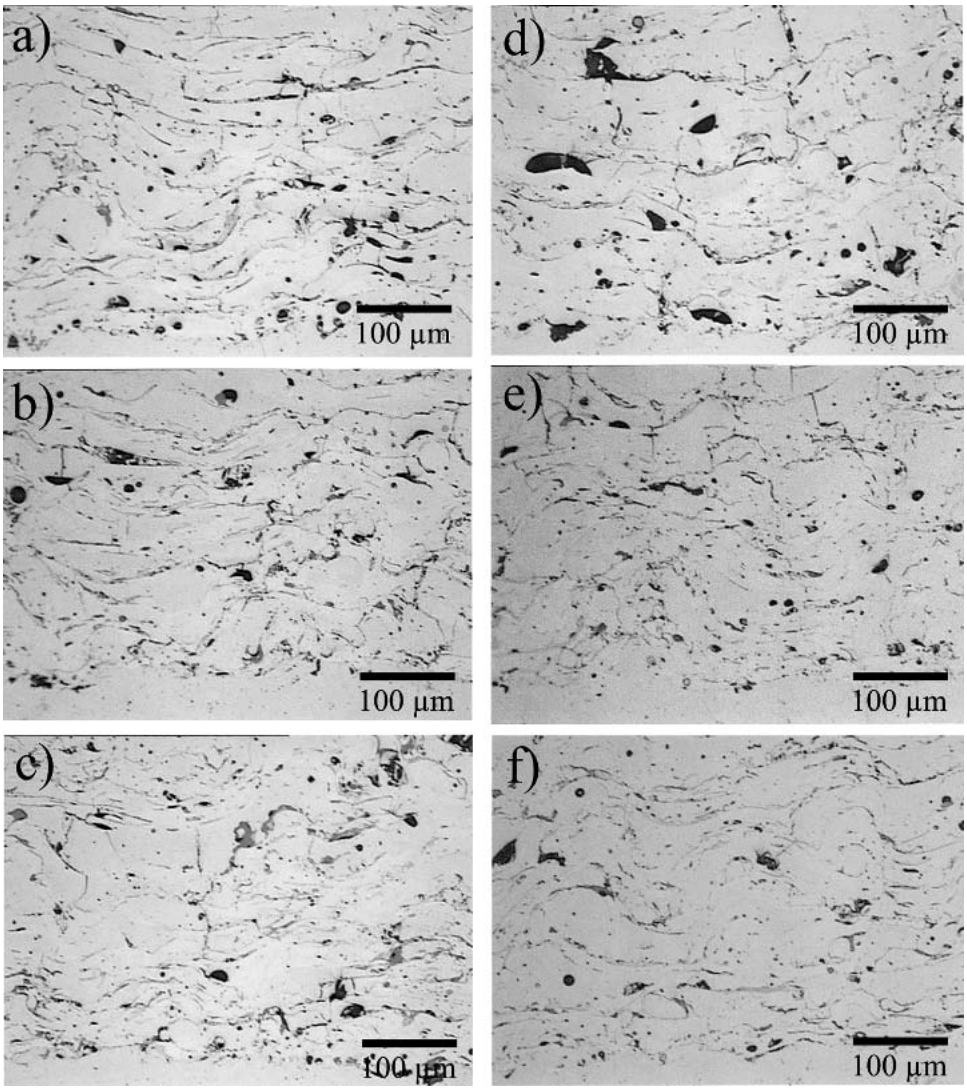

Fig. 6 Optical micrographs showing the change in macrostructure of the coating as a function of spray conditions: (a) 75° at a 12.7 cm stand off, (b) 60° at a 12.7 cm stand off, (c) 45° at a 12.7 cm stand off, (d) 90° at a 7.62 cm stand off, (e) 90° at a 10.16 cm stand off, and (f) 90° at a 15.24 cm stand off

turnaround. All of this makes quality and quality control a real problem, which can result in premature coating failure leading to an unexpected boiler shutdown. Therefore, it is very important that the spray materials and processes exhibit very good forgiveness toward application conditions and variations in spraying parameters. While good-quality coatings can be created in many materials in the laboratory, field applications, especially in boilers, can often result in poor coatings. To study the sprayability of the SHS7170 cored wire, a study was launched to show the influence of spray distance and spray angle on the coating properties as a method for simulating the application of the coating material to an actual boiler.

3.3.1 Spraying Angle Influence. A set of coupons was sprayed at a constant stand off distance with the spray angle at four different values. Micrographs of the cross sections of the 75°, 60°, and 45° as-sprayed coatings are shown in Fig. 6(a) to (c), and reveal very little difference in structure as a function of spray angle. For each sample, the porosity, microhardness, superficial hardness, and deposit efficiency were determined, and the results are summarized in Table 1. The changes in the properties of the coatings as a function of spray angle were found to be insignificant.

3.3.2 Spraying Distance Influence. A set of coupons was sprayed at a constant spray angle with the standoff distance at four different values. Micrographs of the cross sections of the as-sprayed coatings at 7.62, 10.16, 12.7, and 15.24 cm stand off distances are shown in Fig. 6(d) to (f), and reveal very little difference in structure as a function of spray distance. For each sample, the porosity, microhardness, superficial hardness, and deposit efficiency were determined, and the results are summarized in Table 2. The changes in the properties of the coatings as a function of spray distance are found to be inconsequential.

3.3.3 Coating Repairability. Thermal spray coatings are sacrificial, and even when performing well in boilers they will still need to be reapplied during the lifetime of most boilers. Thus, the ability of a coating to be repaired and recoated is cru-

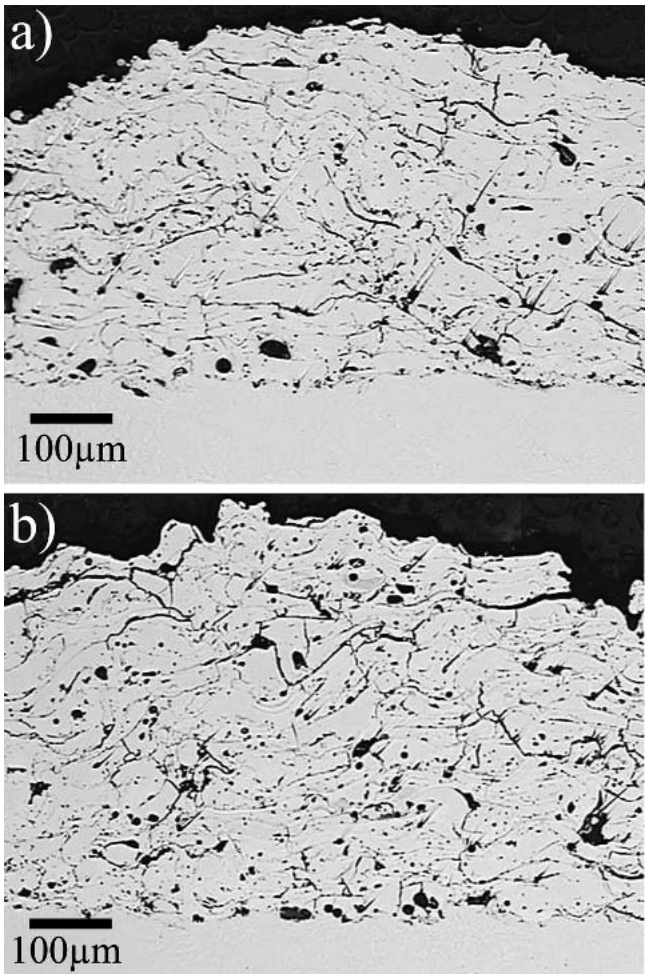

Fig. 7 Optical micrograph showing the repaired (a) and "tie in" (b) cross section of the SHS7170 coatings. Note the interface is approximately in the middle of each image yet it cannot be identified indicating that the coatings are homogeneous after each repairability test.

cial to the success of the protection system during the lifetime of the particular application. To study this, two separate studies were done on 0.0508 cm thick SHS7170 wire-arc coatings to mimic both a coating repair procedure and a coating tie-in procedure.

During both the repair and tie-in procedures, no delamination, cracking, or other specific defects were observed. Examples of the cross sections of both the repaired and tie-in coatings are shown in Fig. 7. Both the repaired and tie-in areas exhibit similar structures and interfaces, as observed in the as-sprayed SHS7170 coating. During analysis of these areas, only a local thickness increase near the masking line allows the discovery of the edge of the stripped coating. The ability to repair the 0.0508 cm thick coating is superior to what is commonly found in other wire-arc materials.

3.3.4 Ash Properties. Samples of the same lot of feedstock bed ash were used for all of the high-temperature erosion tests, and consisted of particles that were mainly angular in shape with a particle size ranging from 63 to 1700 μm, a mean particle size of 566 μm, and a mean particle density of 2522 kg/m^3. Using EDS analysis, the particles of bed ash were found to contain

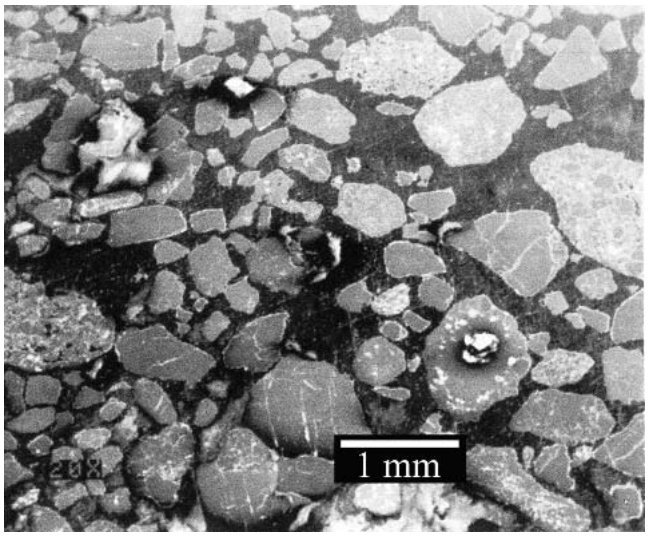

Fig. 8 SEM micrograph representative of the bed ash used for the elevated temperature erosion experiments

oxide particles with high concentrations of Si, and minor concentrations of Al, Ca, S, Fe, K, Ti, and Cl. This compositional analysis is consistent with the normal constituents of ash (SiO_2, Al_2O_3, CaO, SO, Fe_2O_3, KO_2, and TiO_2), which have been identified elsewhere (Ref 3). Notice that while fly ash contacts with higher velocity, it is smaller in size and generally less erosive than bed ash. The hot erosion tests were carried out at three temperatures (300, 450, and 600 °C) under identical test conditions using the more erosive bed ash with a particle velocity of 60 m/s and 375 g particle loading (Ref 3).

3.3.5 Elevated-Temperature Erosion. Elevated-temperature erosion studies were done on SHS7170 wire-arc coupons at three different test temperatures (300, 450, and 600 °C). Examples of the bed ash that was used for the erosion tests can be seen in Fig. 8. Additionally, comparative data are presented on some existing commercial wire-arc coatings, including TAFA 95MXC and Inconel 625, and are compared with 1018 steel plate measured under identical test conditions. For each sample, erosion tests were conducted at both 30° and 90° impact angles, and at a total test time of 5 h at the test temperature. Thickness loss and weight loss were measured on all specimens. Because the weight measurements included the material erosion wastage (−) along with the remaining oxide scale (+) and ash deposition (+), the thickness change was found to be the more valid measurement of material wastage. This was especially true at 600 °C where extensive oxidation occurred in the base 1018 steel material and often resulted in a net positive weight gain.

The results of the elevated temperature erosion tests conducted at 300, 450, and 600 °C, respectively, are given in Tables 4, 5, and 6. The results show that the SHS7170 wire-arc coatings generally exhibit better erosion resistance at low impact angles. This is consistent with the high hardness of the coating and its ability to resist the cutting or ploughing mechanism of impinging particles impacting at low angles. At high angles, the kinetic energy of the impinging particles is transferred directly to the coating, and material removal occurs by the formation of cracks. Notice that in contrast to ceramic coatings, which perform far

Table 4 Elevated temperature erosion at 300 °C

	Weight loss, g		Thickness loss, μm	
Material	**α = 30°**	**α = 90°**	**α = 30°**	**α = 90°**
SHS7170 wire-arc coating	4.0	6.1	26	36
95MXC wire-arc coating	6.3	6.5	35	47
1018 steel plate	44.5	18.3	218	118

Table 5 Elevated temperature erosion at 450 °C

	Weight loss, g		Thickness loss, μm	
Material	**α = 30°**	**α = 90°**	**α = 30°**	**α = 90°**
SHS7170 wire-arc coating	2.8	6.7	32	47
95MXC wire-arc coating	6.7	9.1	36	49

Table 6 Elevated temperature erosion at 600 °C

	Weight loss, g		Thickness loss, μm	
Material	**α = 30°**	**α = 90°**	**α = 30°**	**α = 90°**
SHS7170 wire-arc coating	+4.6	+4.4	36	49
95MXC wire-arc coating	+5.6	+4.1	42	53
Inconel 625 wire-arc	6.2	4.2	142	123

better at low impact angles, or ductile metals, which perform better at high angles, the SHS7170 wire-arc only shows a small angular dependence on erosion. This universal ability to resist erosion almost independently of contact angle is important for real-world boiler applications where the angle of impact changes depending on the area of the boiler, its design, and the amount of turbulent/lamellar flow. Additionally, it is found that an increase in the erosion rate of roughly 20% to 30% occurs when the erosion temperature increases from 300 to 450 °C, but that an increase of only a 4% to 12% occurs on increasing the temperature from 450 to 600 °C. An alternative alloy (Alpha 1800) shows an increase in erosion rate of about 25% at temperatures from 300 to 450 °C, but shows an increase of 220% on increasing the temperature from 450 to 600 °C when tested in air with a much smaller erodent particle size (Ref 21). This beneficial increase in performance at elevated temperatures is probably due to the glass content of the coating crystallizing and becoming harder with increasing temperature. Thus, the SHS7170 nanocomposite coatings provide significant erosion resistance and protection over a wide temperature range. Again, notice that this ability is a result of the temperature stability of the stable nanocomposite structure that is formed as a result of the glass devitrification transformation.

At 300 °C, the comparison between the SHS7170 wire-arc coatings and the base 1018 steel plate clearly shows an increase in the lifetime performance of the wire-arc coatings from 227% to 740% over that of the base steel, depending on impact angle. Because coatings can be recoated in situ while damaged steel pipe will need to be replaced, the advantages of using SHS7170 wire-arc coatings are compelling, especially when considering both the costs of replacing the base steel heat-exchange pipes and the extended downtimes resulting from an unexpected shutdown. At all temperatures, the SHS7170 wire-arc coatings were found to be superior and to have less erosion thickness loss compared with the 95MXC wire-arc coatings that are commonly used for low-temperature boilers. At elevated temperatures, due to the more severe corrosion environment, Inconel 625 wire-arc coatings often are used. At 600 °C, the Inconel 625 wire-arc coatings were found to exhibit a 150% to 290% increase in thickness loss, depending on the contact angle, compared with the SHS7170 wire-arc coatings.

4. Conclusions

In this article, results are clearly presented showing the advantages of using the newly developed SHS7170 wire-arc coatings to provide elevated-temperature erosion protection for boilers in corrosive environments. The compelling properties observed result from the ability to develop nanoscale composite microstructures in air using conventional wire-arc spray guns. The ability to spray the SHS7170 wire-arc coatings in the field has been demonstrated, because the coating is found to be easy to apply with a wide processing window and very good spray forgiveness, and, once coated, is easily recoated and repaired. While there are many different types of coating materials with different combinations of properties, all coatings can only provide protection to a component as long as they remain bonded to the component. The SHS7170 coatings are found to excel in this respect, and to exhibit high bond strength along with high toughness and resiliency. The elevated-temperature erosion resistance of the SHS7170 wire-arc coatings was found to be superior based on thickness loss compared with the existing wire-arc coatings that have been tested. The universal ability of the SHS7170 coatings to resist erosion almost independently of contact angle and at temperatures at least up to 600 °C is important for real-world boiler applications, and is one result of its unique and stable nanoscale structure, which is uniform on bulk-length scales.

References

1. Anon., Boiler Enclosures: Casing and Insulation, *Steam: Its Generation and Use,* 40th ed., S.C. Stultz and J.B. Kitto, Ed., Babcock & Wilcox Company, New York, 1992, p 22-42
2. V. Higuera Hidalgo, J. Belzunce Varela, J. Martinex de la Calle, and A. Carriles Menendez, Characterization of NiCr Flame and Plasma Sprayed Coatings for Use in High Temperature Regions of Boilers, *Surf. Eng.,* Vol 16 (No. 5), 2000, p 137-142
3. V. Higuera Hidalgo, F.J. Belzunce Varela, and E. Fernandez Rico, Erosion Wear and Mechanical Properties of Plasma-Sprayed Nickel- and Iron-Based Coatings Subjected To Service Conditions In Boilers, *Tribol. Int.,* Vol 30 (No. 9), 1997, p 641-649
4. T. Grosdidier, H.L. Liao, and A. Tidu, X-ray and TEM Characterization of Nanocrystalline Fe Aluminde Coatings Prepared by High Velocity Oxy-Fuel Thermal Spraying, *Thermal Spray: Surface Engineering via Applied Research,* C.C. Berndt, Ed., May 8-11, 2000 (Montréal, Québec, Canada), ASM International, 2000, p 1341-1344
5. M.L. Lau, E. Strock, A. Fabel, C.J. Lavernia, and E.J. Lavernia, Synthesis and Characterization of Nanocrystalline Co-Cr Coatings by Plasma Spraying, *Nanostruct. Mater.,* Vol 10 (No. 5), 1998, p 723-730
6. V.L. Tellkamp, M.L. Lau, A. Fabel, and E.J. Lavernia, Thermal Spraying of Nanocrystalline Inconel 718, *Nanostruct. Mater.,* Vol 9 (No. 1-8), 1997, p 489-492
7. M.L. Lau, V.V. Gupta, and E.J. Lavernia, Particle Behavior of Nanocrystalline 316-Stainless Steel During High Velocity Oxy-Fuel Thermal Spray, *Nanostruct. Mater.,* Vol 12 (No. 1-4), 1999, p 319-322
8. B.H. Kear and G. Skandan, Thermal Spray Processing of Nanoscale Materials, *Nanostruct. Mater.,* Vol 8 (No. 6), 1997, p 765-769
9. H.G. Jiang, M.L. Lau, and E.J. Lavernia, Grain Growth Behavior of

Nanocrystalline Inconel 718 and Ni Powders and Coatings, *Nanostruct. Mater.,* Vol 10 (No. 2), 1998, p 169-178
10. M.L. Lau, V.V. Gupta, and E.J. Lavernia, Mathematical Modeling of Particle Behavior of Nanocrystalline Ni During Velocity Oxy-Fuel Thermal Spray, *Nanostruct. Mater.,* Vol 10 (No. 5), 1998, p 715-722
11. Y.C. Zhu and C.X. Ding, Plasma Spraying of Porous Nanostructured TiO_2 Film, *Nanostruct. Mater.,* Vol 11 (No. 3), 1999, p 319-323
12. J. Karthikeyan, C.C. Berndt, J. Tikkanen, J.Y. Wang, A.H. King, and H. Herman, Preparation of Nanophase Materials by Thermal Spray Processing of Liquid Precursors, *Nanostruct. Mater.,* Vol 9 (No. 1-8), 1997, p 137-140
13. J. Tikkanen, K.A. Gross, C.C. Berndt, V. Pitkänen, J. Keskinen, S. Raghu, M. Rajala, and J. Karthikuyan, Characteristics of the Liquid Flame Spray Process, *Surf. Coat. Technol.,* Vol 90 (No. 3), 1997, p 210-216
14. N.P. Rao, H.J. Lee, M. Kelkar, D.J. Hansen, J.V.R. Herberlein, P.H. McMurry, and S.L. Girshick, Nanostruct. Mater. Production by Hypersonic Plasma Particle Deposition, *Nanostruct. Mater.,* Vol 9 (No. 1-8), 1997, p 129-132
15. D.J. Branagan, W.D. Swank, D.C. Haggard, J.R. Fincke, Wear Resistant Amorphous and Nanocomposite Steel Coatings, *Metall. Mater. Trans. A,* Vol 32A (No. 10), 2001, p 2615-2621
16. D.J. Branagan, Devitrified Nanocomposite Steel Powder, *Powder Metallurgy Alloys and Particulate Materials for Industrial Application,* D.E. Alman and J.W. Newkirk, Eds., The Minerals, Metals, and Materials Society, Warrendale, PA, 2001, p 111-122
17. D.J. Branagan, M.J. Kramer, and R.W. McCallum, Transition Metal Carbide Formation in the $Nd_2Fe_{14}B$ System and Potential as Alloying Additions, *J. Alloys Compd.,* Vol 244 (No. 1-2), 1996, p 27-39
18. A.V. Levy and Y.F. Man, Erosion-Corrosion of Chromium Steel, *Corrosion-Erosion-Wear of Materials at Elevated Temperatures,* A.V. Levy, Ed., NACE International, Houston, TX, 1986, p 168-203
19. B.B. Kappes, B.E. Meacham, Y.L. Tang, and D.J. Branagan, Relaxation, Recovery, Crystallization, and Recrystallization Transformations in an Iron Based Amorphous Precursor, *Nanotechnology,* Vol 14 (No. 11), 2003, p 1228-1234
20. D.J. Branagan and Y. Tang, Developing Extreme Hardness (>15 GPa) in Iron Based Nanocomposites, *Composites Part A,* Vol 33 (No. 6), 2002, p 855-859
21. S. Dallaire, Hard Arc-Sprayed Coating with Enhanced Erosion and Abrasion Wear Resistance, *J. Thermal Spray Technol.,* Vol 10 (No. 3), 2001, p 511-519